A&A 443, 293–296 (2005)
DOI: 10.1051/0004-6361:20053412

Astronomy & Astrophysics

Non-LTE modelling of the He I 10830 Å line in early-type main sequence stars

N. Przybilla

Dr. Remeis-Sternwarte Bamberg, Universität Erlangen-Nürnberg, Sternwartstrasse 7, 96049 Bamberg, Germany
e-mail: przybilla@sternwarte.uni-erlangen.de

Received 12 May 2005 / Accepted 3 July 2005

ABSTRACT

The near-IR He I 10 830 Å transition is a highly sensitive diagnostic for non-LTE effects in astrophysical plasmas. So far, non-LTE line-formation computations have failed to quantitatively reproduce observations of this line in the entire range of early-A to late-O main sequence stars. It is shown that the non-LTE modelling was insufficient, for the most part, either because of inaccurate photoionization cross-sections for the $2s\,^3S$ state or because of neglecting line blocking. New calculations based on state-of-the-art atomic data give excellent agreement with observation for the He I 10 830 Å feature, while profiles of the He I lines in the visual are retained.

Key words. line: formation – infrared: stars – stars: early-type

1. Introduction

The 10 830 Å transition ($2s\,^3S$–$2p\,^3P^\circ$) in neutral helium is very important for constraining non-LTE effects in the second most abundant element. It involves the metastable state of the triplet spin system and is consequently prone to non-LTE effects, because the triplets are only loosely coupled via collisions to the singlet system. In addition, its location in the Rayleigh-Jeans tail of the energy distribution of hot stars gives rise to amplified non-LTE effects in this class of objects.

Since detection of this line in the solar disk spectrum (Babcock & Babcock 1934), it has been observed in most kinds of stars throughout the Hertzsprung-Russell diagram (HRD). It is widely used as an indicator of chromospheric activity in the Sun and other cool stars (e.g. Zirin 1982). Towards the hot end of the HRD, this feature is observed as a prominent emission line, as in O-stars (e.g. Andrillat & Vreux 1979) and in Wolf-Rayet stars (e.g. Howarth & Schmutz 1992). The He I 10 830 Å transition is also discussed in a galactic and cosmological context, ranging from local gaseous nebulae to Seyfert galaxies and QSOs (e.g. LeVan et al. 1984). The plasma conditions in chromospheres, stellar winds, and gaseous nebulae lead to rather complex physics of the non-LTE line formation (e.g. Avrett et al. 1994; Peimbert & Torres-Peimbert 1987). Therefore it is impossible to separate inaccuracies of input atomic data from shortcomings in the plasma physics model. Consequently it is mandatory to study the transition in a well-understood environment, such as the stellar atmospheres of early-type stars with negligible mass-loss. Main sequence stars of spectral types early-A to late-O are excellent testbeds. However, non-LTE line-formation computations for stars in this region of the HRD (Auer & Mihalas 1972, 1973 – AM72/73; Dufton & McKeith 1980 – DMK80; Leone et al. 1995 – LLP95) have at best reproduced observations (Meisel et al. 1982; Lennon & Dufton 1989 – LD89; LLP95) only qualitatively so far. The present study resolves the issue. Naturally, the findings will have broader implications than for this objective alone.

2. Model calculations

Two He I model atoms are used in the present work: I) the "standard" model of Husfeld et al. (1989), which is a slightly improved version of the AM73 model atom, later updated with collisional excitation data of Berrington & Kingston (1987), and II) an extended "new" version of the Husfeld et al. model. Considering the term structure of the new model atom, the difference is that now all states up to principal quantum number $n = 5$ are treated individually (previously up to $n = 4$), with the remainder grouped into combined levels for each n in the singlet and triplet spin systems. Oscillator strengths are adopted from the NIST database (http://physics.nist.gov/cgi-bin/AtData/main_asd), from Fernley et al. (1987, FTS87), or from the Coulomb approximation, in this order of preference. Photoionization cross-sections of FTS87 are employed, with missing data assumed to be hydrogenic (Mihalas 1978, p. 99). Effective collision strengths for excitation by electron collisions are adopted from ab initio computations of Bray et al. (2000) and Sawey & Berrington (1993). Additional transitions are treated according to Mihalas & Stone (1968), and for the remainder of the optically forbidden transitions, the semiempirical Allen

formula (Allen 1973) is applied. Here collision strengths Ω varying between 0.001 to 1000 are assumed, based on trends derived from examination of the detailed computations of Bray et al. and Sawey & Berrington. The lowest Ω occur for transitions between the ground state and the levels of highest excitation energy, while detailed balance is established between high-lying energy levels due to the large collision rates. Data from Bell et al. (1983) have been adopted for electron impact ionization of the ground state, along with the Seaton (1962) approximation for the other individual levels with threshold photoionization cross-sections from FTS87 where available, or from the hydrogenic approximation. Collisional ionization of the packed levels is accounted for according to Mihalas & Stone (1968). Finally, the theory of Barnard et al. (1969), which is described further in AM72, is utilised for a realistic description of line broadening. The model for He II considers all levels/transitions up to $n = 20$. Its details are of no further importance for the present investigation.

The non-LTE line-formation calculations are performed in a hybrid approach. Based on hydrostatic, plane-parallel, line-blanketed LTE models calculated with the ATLAS9 code (Kurucz 1993), the non-LTE line formation is solved using DETAIL and SURFACE (Giddings 1981; Butler & Giddings 1985). The coupled radiative transfer and statistical equilibrium equations are solved employing an accelerated lambda iteration scheme that uses the treatment of Rybicki & Hummer (1991). Line-blocking is realised by considering Kurucz' opacity distribution functions. Note that microturbulence is explicitly accounted for in the solution of the statistical equilibrium and radiative transfer by inclusion of an additional term in the width of the (depth-dependent) Doppler profiles adopted at that stage of the calculations. The grid comprises models for effective temperature $T_{\rm eff}$ ranging from 10 000 to 35 000 K at a single surface gravity value of $\log g = 4.0$ (cgs), which is adequate for early-type dwarfs with negligible mass-loss. Solar composition is assumed, with the microturbulent velocity ξ fixed to two values of 0 and 8 km s^{-1}. Theoretical reddening-free Strömgren $[c_1]$-indices (where $[c_1] = c_1 - 0.2(b-y)$) are determined for the ATLAS9 model atmospheres using the suite of programs for synthetic photometry by Kurucz. The $[c_1]$-index parameterises the effective temperature for the comparison with observation.

The computed He I/II lines at visual wavelengths in several of the hotter models ($27\,500 \leq T_{\rm eff} \leq 35\,000$ K) have been compared with state-of-the-art non-LTE model atmosphere calculations of Lanz & Hubeny (2003, LH03). Excellent agreement is found for the He I triplets and He II lines (and also the hydrogen Balmer lines) except for the utmost line cores, indicating that non-LTE effects on the atmospheric structure are small at line-formation depths and confirming the validity of the hybrid approach. The present computations predict stronger He I singlets than LH03, with the discrepancy increasing with decreasing surface gravity. Note that the present modelling gives better agreement with the observed visual spectrum of the standard star τ Sco. The He I 10 830 Å feature is not included in the spectrum synthesis of LH03.

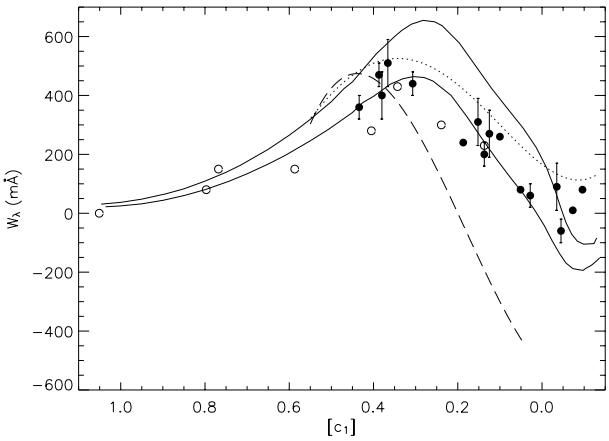

Fig. 1. Comparison of observed equivalent widths for He I 10830 Å (Lennon & Dufton 1989: filled circles; Leone et al. 1995: open circles) with model predictions: Auer & Mihalas (1973, dotted line), Dufton & McKeith (1980, dashed line), and present computations (full lines) for $\xi = 0$ (*lower*) and 8 km s^{-1} (*upper curve*). The abscissa is the reddening-free $[c_1]$ index. Measurements of LD89 without error bars have uncertainties >80 mÅ. Uncertainties for the fast rotators of the LLP95 sample can be well above 100 mÅ.

3. Comparison with observation

New non-LTE line-formation computations have to prove their worth by improving the model predictions when confronted with observation. Spectroscopic investigations of the He I 10 830 Å transition in early-type main sequence stars are scarce, because of the reduced flux of this type of star, contamination of the spectra by telluric absorption at these wavelengths, and low sensitivity of standard CCDs in the J band. Only two sources of measurements of equivalent widths W_λ from observations with modern instrumentation are available from the literature: a sample of 16 slow-rotating ($v \sin i \lesssim 30$ km s^{-1}) B6–O9 stars from LD89 and 8 normal A1 to B2 dwarfs and subgiants from LLP95 (their chemically peculiar objects are omitted in the following), almost all of them being fast rotators ($v \sin i \gtrsim 130$ km s^{-1}). Both samples have γ Peg in common, for which satisfactory agreement of the equivalent width is found.

A comparison of equivalent widths from the present non-LTE computations with observation is made in Fig. 1, where previous model predictions are also summarised, employing the same $[c_1]$ calibrations as in LD89. As already found by LD89, the calculations of AM73 systematically predict too strong equivalent widths for He I 10 830 Å, while those of DMK80 indicate that this line goes from absorption into (strong) emission near spectral type B2. Their calculations do not cover effective temperatures below 15 000 K. Hybrid non-LTE computations based on line-blanketed ATLAS9 atmospheres by LLP95 (not shown) find good agreement in the cooler stars, and a qualitatively similar behaviour as DMK80 predicting slightly less pronounced emission for spectral types earlier than B2. Observation, on the other hand, indicates a maximum of equivalent widths around spectral type B2, levelling off towards the late-O stars and eventually leading to small emission, as is the case in τ Sco. Consequently, none

of the non-LTE line-formation computations for He I 10 830 Å from the literature reproduce the trend in observed equivalent width of dwarf stars over the whole range of spectral types from early-A to late-O.

The new calculations succeed here, finding excellent agreement with observations, as can be seen in Fig. 1. Note that the principal error in equivalent width measurements comes from continuum placement, such that the uncertainties can be expected to be largest in the fast rotators of the LLP95 sample. A correct location of the maximum of line strength is indicated and much weaker emission than in previous cases, reaching a maximum at $T_{\rm eff} \simeq 31\,000$ K. The emission is reduced for higher microturbulent velocities and levels off towards higher temperatures as helium becomes ionized. The observational trends imply near-solar helium abundances and low microturbulent velocities in the cooler stars and enhanced helium and/or higher microturbulences for the earlier types (the more massive objects). This agrees well with the findings from analyses of early B-stars in the classical visual wavelength range (e.g. Lyubimkov et al. 2004) and predictions from recent stellar evolution calculations (e.g. Heger & Langer 2000; Meynet & Maeder 2000). The results are reassuring; however, the reasons for the improvements in the predictions need to be understood quantitatively. This is investigated in the following.

4. Discussion

A comparison of the predictions from several non-LTE calculations is made for atmospheric parameters typical of an early B-type main sequence star. The computations are based on both the standard and the new model atom, and a version of the latter where the photoionization cross-section for the $2s\,^3S$ state is replaced by the one used in the old model atom. Departure coefficients $b_i = n_i/n_i^*$ (the n_i and n_i^* being the non-LTE and LTE populations of level i, respectively) for the $n = 1$ and 2 levels of He I are displayed in Fig. 2. Excellent agreement is found, except for the $2s\,^3S$ state (and minor differences for the $2p\,^3P^o$ level). The new model atom predicts level populations by up to ∼10% lower at line-formation depths than the other two models, which mutually deviate much less.

Because of the high sensitivity of the line-source function S_l to variations of the departure coefficients in the Rayleigh-Jeans limit (see e.g. Przybilla & Butler 2004), this relatively small difference in level populations can result in fundamentally altered line strengths for He I 10 830 Å. While a ratio of S_l/B_ν (B_ν being the Planck function) slightly larger than unity in the old model atom (and the modified new one) leads to reduced absorption when compared to detailed balance predictions, the significantly larger values in the new model give net emission (see Fig. 3). This is primarily because of the considerable difference in the photoionization cross-sections for the metastable state, the FTS87 data being considerably larger, by more than 50% at threshold, see Fig. 4. This weakness in the AM73 work has already been pointed out by DMK80, but see also LD89. Note that the detailed resonance structure of the FTS87 cross-sections, which are constrained to a narrow region at short wavelengths, are not accounted for in the current computations.

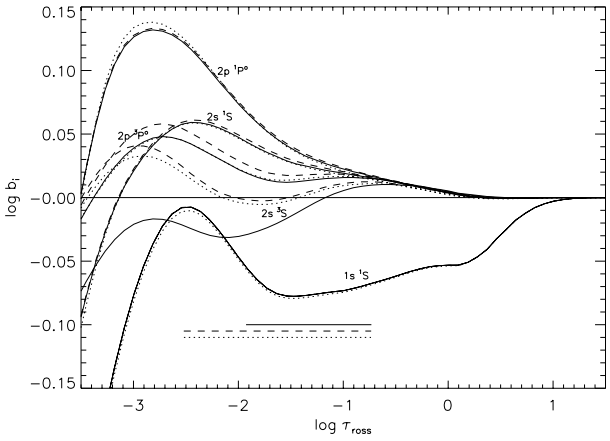

Fig. 2. Comparison of departure coefficients b_i as a function of Rosseland optical depth $\tau_{\rm ross}$ for the $n = 1$ and 2 levels of He I from computations using the standard (dotted lines) and the present (full lines) model atom, and computations for the new model atom with the photoionization cross-section for the $2s\,^3S$ state replaced by that used in the old one (dashed lines). Good agreement is found except for the $2s\,^3S$ state, the lower level of the He I 10 830 Å transition. Line-formation depths for this feature are indicated. The computations are for a stellar atmospheric model with $T_{\rm eff} = 30\,000$ K, $\log g = 4.0$ (cgs), zero microturbulence, solar metallicity, and solar helium abundance.

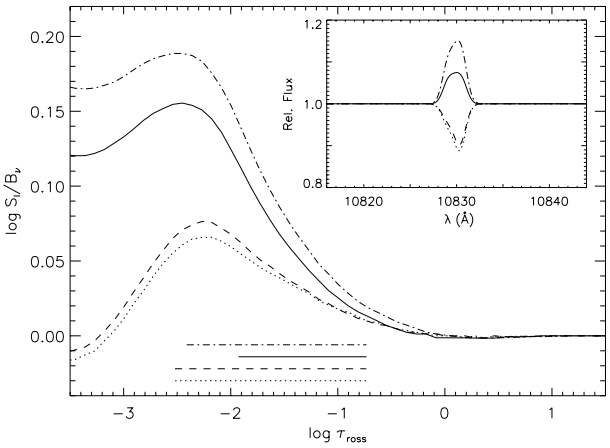

Fig. 3. Ratio of the line source function S_l to Planck function $B_\nu(T)$ at the centre of the 10 830.34 Å fine-structure component of the transition, for the same atmospheric parameters as in Fig. 2. The same line designations as in Fig. 2 apply. In addition, results from a computation using the new model atom, but neglecting line blocking (dashed-dotted lines), are also shown. In the inset the resulting line profiles are compared after convolution with a Gaussian of *FWHM* of 20 km s^{-1}. Use of the improved photoionization cross-sections turns the absorption into emission, while neglect of line blocking effects gives excess emission.

The importance of *line-blanketed* model atmospheres on the formation of He I 10 830 Å (despite general systematic effects on the atmospheric structure through a steepened temperature gradient) is less pronounced than indicated by LD89, as LLP95 and the present study use the same model atmospheres. In fact, the difference between the DMK80 and LLP95 studies, on the one hand, and ours on the other, is the allowance for *line blocking*. We therefore computed an additional model

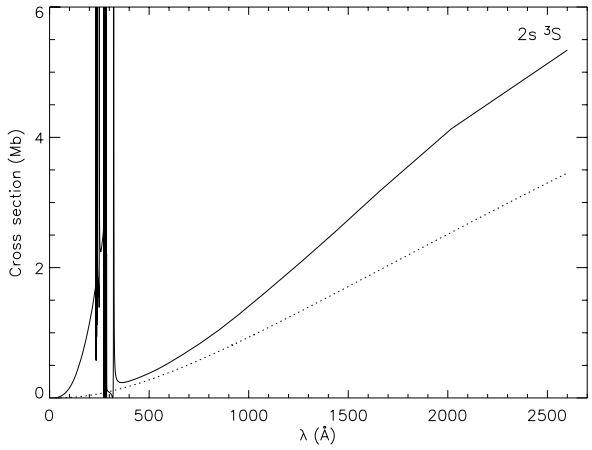

Fig. 4. Comparison of the photoionization cross-sections for the $2s\,^3S$ state of Fernley et al. (1987, full line), as used in the present He I non-LTE model atom and of Gingerich (1964, dotted line), as used in the AM73 and Husfeld et al. (1989) models. The cross sections differ by more than 50% at threshold.

neglecting line blocking as in the older work. Much larger emission results from this, enhanced by a factor ∼2 in the case discussed in Fig. 2. This is facilitated by significantly larger ionization of He I by the unblocked UV-radiation, which gives (markedly) lower non-LTE populations for the ground state and the $n = 2$ levels. In particular, the $2s\,^3S$ state experiences stronger depopulation relative to $2p\,^3P^\circ$, giving rise to the stronger emission in He I 10 830 Å in the hotter stars. The agreement of the LLP95 computations with observation for the cooler stars is also explained in this picture, as photoionization of He I is inefficient there. Note that the profiles of the He I lines in the visual are largely insensitive to the effects of line blocking.

5. Conclusions

The present study resolves long-standing discrepancies between non-LTE computations and observations for the He I 10 830 Å transition in early-type main sequence stars. Excellent quantitative agreement is indicated now on the level of accuracy of equivalent width measurements from the literature. Earlier non-LTE analyses suffered from inaccurate photoionization cross-sections for the $2s\,^3S$ state and/or neglected line blocking. The profiles of the He I lines in the visual are largely insensitive to these details.

Further efforts for constraining non-LTE effects for helium are nonetheless required, as the quantitative interpretation of a wide range of astronomical objects relies on accurate line-formation computations for this element. These should consider high-S/N and high-resolution observations including the complete near-IR range as facilitated by modern telescopes and instrumentation. Line-profile information for all available indicators will allow stringent constraints to be put on the He I model atom.

Acknowledgements. I wish to thank K. Butler for valuable suggestions and careful reading of the manuscript.

References

Allen, C. W. 1973, Astrophysical Quantities, 3rd edition (London: Athlone Press)
Andrillat, Y., & Vreux, J. M. 1979, A&A, 76, 221
Auer, L. H., & Mihalas, D. 1972, ApJS, 24, 193 (AM72)
Auer, L. H., & Mihalas, D. 1973, ApJS, 25, 433 (AM73)
Avrett, E. H., Fontenla, J. M., & Loeser, R. 1994, in Infrared Solar Physics, ed. D. M. Rabin, J. T. Jefferies, & C. Lindsey (Dordrecht: Kluwer), 35
Babcock, H. D., & Babcock, H. W. 1934, PASP, 46, 132
Barnard, A. J., Cooper, J., & Shamey, L. J. 1969, A&A, 1, 28
Bell, K. L., Gilbody, H. B., Hughes, J. G., Kingston, A. E., & Smith, F. J. 1983, J. Phys. Chem. Ref. Data, 12, 891
Berrington, K. A., & Kingston, A. E. 1987, J. Phys. B, 20, 6631
Bray, I., Burgess, A., Fursa, D. V., & Tully, J. A. 2000, A&AS, 146, 481
Butler, K., & Giddings, J. R. 1985, in Newsletter on Analysis of Astronomical Spectra, No. 9 (London: Univ. London)
Dufton, P. L., & McKeith, C. D. 1980, A&A, 81, 8 (DMK80)
Fernley, J. A., Taylor K. T., & Seaton M. J. 1987, J. Phys. B, 20, 6457 (FTS87)
Giddings, J. R. 1981, Ph.D. Thesis, Univ. London
Gingerich, O. 1964, in Proc. 1st Harvard-Smithsonian Conf. Stellar Atmospheres, SAO Spec. Rep., 167 (Cambridge: SAO), 17
Heger, A., & Langer, N. 2000, ApJ, 544, 1016
Howarth, I. D., & Schmutz, W. 1992, A&A, 261, 503
Husfeld, D., Butler, K., Heber, U., & Drilling, J. S. 1989, A&A, 222, 150
Kurucz, R. L. 1993, Kurucz CD-ROM, No. 13 (Cambridge, Mass.: Smithsonian Astrophysical Observatory)
Lanz, T., & Hubeny, I. 2003, ApJS, 146, 417 (LH03)
Lennon, D. J., & Dufton, P. L. 1989, A&A, 225, 439 (LD89)
Leone, F., Lanzafame, A. C., & Pasquini, L. 1995, A&A, 293,457 (LLP95)
LeVan, P. D., Puetter, R. C., Smith, H. E., & Rudy, R. J. 1984, ApJ, 284, 23
Lyubimkov, L. S., Rostopchin, S. I., & Lambert, D. L. 2004, MNRAS, 351, 745
Meisel, D. D., Saunders, B. A., Frank, Z. A., & Packard, M. L. 1982, ApJ, 263, 759
Meynet, G., & Maeder, A. 2000, A&A, 361, 101
Mihalas D. 1978, Stellar Atmospheres, 2nd edition (San Francisco: W. H. Freeman and Company)
Mihalas, D., & Stone, M. E. 1968, ApJ, 151, 293
Peimbert, M., & Torres-Peimbert, S. 1987, Rev. Mex. Astron. Astrofis., 15, 117
Przybilla, N., & Butler, K. 2004, ApJ, 609, 1181
Rybicki, G. B., & Hummer, D. G. 1991, A&A, 245, 171
Sawey, P. M. J., & Berrington, K. A. 1993, At. Data Nucl. Data Tables, 55, 81
Seaton, M. J. 1962, in Atomic and Molecular Processes (New York: Academic Press)
Zirin, H. 1982, ApJ, 260, 655